Наносистеми, наноматеріали, нанотехнології
Nanosistemi, Nanomateriali, Nanotehnologii
2020, т. 18, № 4, сс. 983–1001

PACS numbers: 61.80.Ba, 68.37.Hk, 78.20.Ci, 78.67.Sc, 81.07.Pr, 82.35.Np, 85.60.Gz

Structural and Optical Properties of (PMMA/ZrO_2/Ag) New Nanocomposites for Optoelectronics and UV Detectors Applications

Angham Hazim[1], Ahmed Hashim[2], and Hayder M. Abduljalil[1]

[1]*University of Babylon,*
College of Science,
Department of Physics,
Babylon, Iraq
[2]*University of Babylon,*
College of Education for Pure Sciences,
Department of Physics,
Babylon, Iraq

In this paper, structural and optical properties of PMMA–ZrO_2 nanocomposites doped with silver nanoparticles are investigated. The silver nanoparticles are added to PMMA–ZrO_2 nanocomposites with concentrations of 2, 4 and 6 wt.%. The experimental results show that the absorption coefficient, extinction coefficient, refractive index, dielectric constants, and optical conductivity of PMMA–ZrO_2 nanocomposites are increased, while both the transmittance and the energy band gap are decreased with increase in silver-nanoparticles' concentration. The obtained results for the structural and optical properties show that the PMMA/ZrO_2/Ag nanocomposites can be used for different medical and industrial applications such as solar cells, diodes, sensors, UV-detectors, *etc*.

У цій роботі досліджуються структурні й оптичні властивості нанокомпозитів PMMA–ZrO_2, оброблюваних наночастинками срібла. Наночастинки срібла додаються до нанокомпозитів PMMA–ZrO_2 з концентраціями 2, 4 і 6 ваг.%. Експериментальні результати показують, що коефіцієнт поглинання, коефіцієнт екстинкції, показник заломлення, діелектричні константи й оптична провідність нанокомпозитів PMMA–ZrO_2 збільшуються, в той час як прозорість та заборонена зона енергій зменшуються зі збільшенням концентрації наночастинок срібла. Одержані результати для структурних і оптичних властивостей показують, що нанокомпозити PMMA/ZrO_2/Ag можуть використовуватися для різних медичних та індустріальних застосувань, таких як сонячні елементи, діоди, датчики, детектори ультрафіолету тощо.

Key words: ZrO_2, PMMA, silver, nanocomposites, optical properties, energy gap.

Ключові слова: ZrO_2, поліметилметакрилат, срібло, нанокомпозити, оптичні властивості, енергетична щілина.

(Received 14 March, 2020; in final version, 1 April, 2020)

1. INTRODUCTION

In latest years, the expansion of new polymers, blends, composites and progressing materials becomes necessity for modification of mechanical, electrical, optical and thermal properties to fulfil the desired features. The expansion runs parallel with intense series of studies aiming to enlighten the structure–property relationship of the revised materials [1]. The optical, electrical, and thermal features of new polymeric films are essential for the development of these films. Transparent films can be hired as optical filters, polarizers, total reflectors, narrow pass-band filters, *etc*. Films of dielectric materials have been successfully utilized in certain optical devices and materials [2]. Integration of macro and nanocomposites has led to the development of a new class of nanocomposite materials, which find vital approach in medicine, biology, industry and defence.

Polymers and organic materials have been receiving a great deal of attention for their unique features offering to realize lightweight, environmental friendly, flexible and cost effective electronic devices [3–5]. Polymethylmethacrylate (PMMA) is one of the important transparent thermoplastic plastics, which has been utilized to make windows, lenses, and other optical devices and used to improve the mechanical properties and process ability of PANI. PMMA is chosen as a dielectric matrix because of its high transparent ability in the visible spectral range, which is important for optoelectronics, sensors, and smart-window applications [6–8]. Polymers and particularly hybrid (organic–inorganic) composites are attracting increasing attention from researchers due to their use in many manufacturing sectors. Introducing metal oxides like ZrO_2 into organic matrices offers more high physical and chemical stability. Inorganic nanoparticles as filler and organic polymers as matrices can endow the resulting nanocomposites with excellent electrical, optical, and mechanical properties [9–13]. These nanocomposites exhibit the merits of blending the advantageous properties of metal oxides with the process ability and flexibility of polymers. Among the most important metal oxides, ZrO_2 (zirconia) is a material of great technological importance, having good natural colour, high strength, transformation toughness, high chemical stability, excellent corrosion resisting material, and chemical and microbial resistance [14–17]. Zirconium oxide ZrO_2 is a wide band gap *p*-type semiconductor that exhibits abundant oxygen vacancies on its surface.

The high ion exchange capacity and redox activities make it useful in catalysis. Zirconium oxide ZrO_2 is also an important dielectric material for potential application as an insulator in transistors in future nanoelectronic devices [18–20]. ZrO_2 nanoparticles have found uses in solid oxide fuel cells and in nitrogen oxide, oxygen gas sensors. The fully stabilized ZrO_2 nanoparticles are also well suited for high-temperature energy conversion systems, attributed to its high oxygen-ion transport capabilities and long-thermostability. Composites are widely utilized our day-to-day life [21–23]. Because of their low weight and ability to be tailored for specific end use they have gained a considerable ground in the high execution applications, like aerospace and automobile industry.

The idea of connecting two or more various constituents into on substance grant almost infinite possibilities to make new engineering materials recognized by variety of different properties. Composite materials because of these diverse properties are successfully used in almost all areas of industry and science [24]. One advantage of nanoparticles, as polymer additives appear to have is that compared to traditional additives, loading necessities are quite low [25].

Microsize particles used as reinforcing agents scatter light, therefore reducing light transmittance and optical clarity. The efficient nanoparticle dispersion combined with good polymer–particle interfacial adhesion eliminates the scattering and allows the exciting possibility of developing strong yet transparent films, coatings and membranes [26]. The optical properties of polymers constitute important aspects in study of electronic transition and the possibility of their application as optical filters, a cover in solar collection, selection surfaces and green house. The information about the electronic structure of crystalline and amorphous semiconductors has been mostly accumulated from the studies of optical properties in wide frequency range [27]. The composites and nanocomposites have huge applications as humidity sensors [28–32], radiation shielding [33–38], antibacterial [39, 41] and thermal energy storage and release [42–46]. The adding of biomaterial, micro- or nanoparticles to the polymer or polymer blend aims to improve in optical properties [47–54], dielectric and electrical properties [55–62]. The aims of current paper, a study the impact of silver (Ag) nanoparticles on structural and optical of (PMMA–ZrO_2) nanocomposites.

2. MATERIALS AND METHODS

The nanocomposites of (PMMA–ZrO_2–Ag) are prepared by dissolving (0.98 gm) of PMMA with (0.02 gm) of ZrO_2, and the Ag nanoparticles are added to ($PMMA-ZrO_2$) nanocomposites with different concentrations of 2, 4 and 6 wt.% dissolved in beaker 20 ml of chloroform using magnetic stirrer to mix the polymer and nanoparticles 30 min to achieve more homogeneous solution. The casting method is used to prepare the specimen of ($PMMA-ZrO_2-Ag$) nanocomposites placed in Petri dish 10 cm diameter. The optical properties of ($PMMA-ZrO_2-Ag$) nanocomposites were recorded for wavelength (220–820) nm using the spectrophotometer double beam (Shimadzu, UV-1800 A). Optical properties of materials are very important due to it can achieve information about the internal structure, the nature of the bonds and their employment by knowing the amount of absorbance, reflectance and transmittance of these materials [63].

By using Lambert's law, it can be calculated the absorption coefficient, which states that absorbance of a material sample is directly proportional to its thickness (path length) (t), and it can be written as follows:

$$\frac{I}{I_0} = e^{-\alpha t}, \tag{1}$$

where (I/I_0)—the ratio of the transmittance intensity of the incident wave to the incident intensity of the same wave, which represents the transmittance of the electromagnetic wave (T) and because the absorbance (A) written as:

$$A = \log\frac{I}{I_0}. \tag{2}$$

The absorption coefficient α can be calculated from the absorption data as [64]

$$\alpha = 2.303\frac{A}{t}, \tag{3}$$

where α is the absorption coefficient for higher photon energies. The simplified general equation is [65]

$$ah\nu = B(h\nu - E_g)^m, \tag{4}$$

where B is a constant; $h\nu$ is the photon energy; E_g is the energy band gap, and m is the parameter connected with distribution of the density of stales. The index $m = 1/2$ for allow direct transition energy gap, and $m = 2$ for indirect transition one [66–69]. Thus, from the straight-line plots of $(\alpha h\nu)^2$ *versus* $h\nu$ and $(\alpha h\nu)^{1/2}$ *versus* $h\nu$, the direct and indirect energy gaps of insulators and/or dielectrics can be determined. The Beer–Lambert law has implicit assumptions that must be met experimentally for it to apply; otherwise, there is a possibility of deviations from the law to be observed [70].

The refractive index represents the ratio of the electromagnetic wave speed in vacuum to the electromagnetic wave speed inside the material. Equation (5) gives the law used to calculate the refractive index [71]:

$$n = \sqrt{\frac{4R - K^2}{(R-1)^2}} - \frac{R+1}{R-1}, \tag{5}$$

where R is the reflectance, which can be calculated in terms of the absorption and the transmission from the energy conservation law [72]:

$$R = 1 - A - T. \tag{6}$$

Complex refractive index can be written as follows:

$$n^* = n - ik, \tag{7}$$

where n is the real part of refractive index; K is the extinction coefficient represents the imaginary part; n^* is a complex number represent the complex refractive index that depends on several characteristic factors such as crystal defect and crystal structure. The extinction coefficient represents the amount of attenuation of an electromagnetic wave that is traveling in a material, where it values depends on the density of free electrons in the material and on the structure nature, this coefficient can be calculated by using the following equation [73]:

$$k = \alpha\lambda/(4\pi), \tag{8}$$

where λ is the wavelength. The extinction coefficient (k) is directly proportional to the absorption coefficient as seen from Eq. (8).

The complex dielectric constant ($\varepsilon^* = \varepsilon_1 + i\varepsilon_2$) characterizes the optical properties of the solid material, where real part (ε_1) and imaginary part (ε_2) of the dielectric constant, and can be calculated by the following relations [74]:

$$\varepsilon_1 = n^2 - k^2, \tag{9}$$

$$\varepsilon_2 = 2nk. \tag{10}$$

The real (ε_1) and imaginary (ε_2) parts of the dielectric constant are related to (n) and (k) values as seen from Eq. (9) and Eq. (10). The calculation of these two parts supplies information about the loss factor.

The optical conductivity has been determined by [75]

$$\sigma = \alpha nc/(4\pi). \tag{11}$$

3. RESULTS AND DISCUSSION

The optical properties of (PMMA–ZrO_2–Ag) nanocomposites involve the absorbance, transmittance, the absorption coefficient, energy band

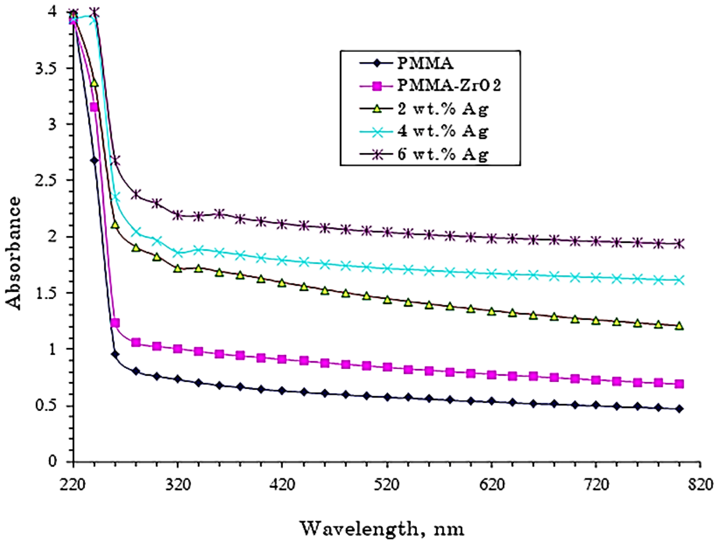

Fig. 1. Absorbance as a function of wavelength for (PMMA–ZrO_2–Ag) nanocomposites.

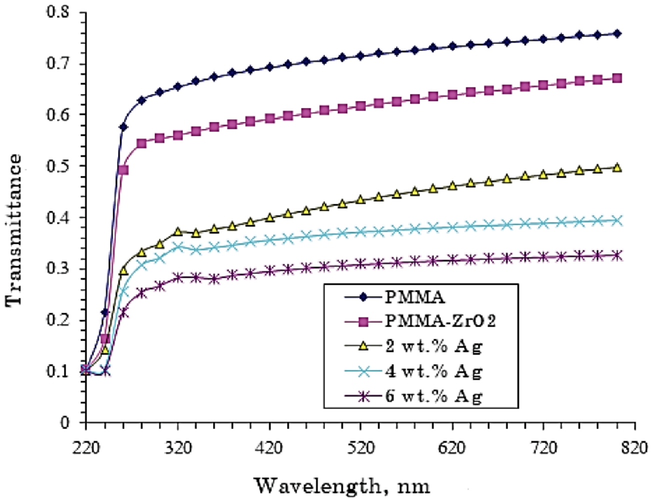

Fig. 2. Transmittance as a function of wavelength for (PMMA–ZrO_2–Ag) nanocomposites.

gap, extinction coefficient, reflection index, dielectric constants, and optical conductivity.

From equation (2), it can be measured the absorbance of (PMMA–ZrO_2–Ag) nanocomposites. Figure 1 shows the absorbance as function of the wavelength of the incident light for (PMMA–ZrO_2) with deferent concentration of Ag. It is observed from figure that the absorption for all specimens of nanocomposites was taken high value near the absorption edge 220 nm UV region with the increasing of the concentrations for Ag nanoparticles. This is because of the excitations of valance band to the conduction band at these energies. At UV region, the high absorbance of specimen for (PMMA–ZrO_2–Ag) nanocomposites assigned to the energy of photon enough to interact with atoms; the electron excites from a lower to higher energy level by absorbing a photon of known energy [76–80].

The absorbance of all specimens for (PMMA–ZrO_2–Ag) nanocomposites at visible and near-infrared regions has low values; this behaviour assigned to the energy of incident photons does not enough energy to interact with atoms. Therefore, the photons will transmit if the wavelength increases [81].

The optical transmittance is defined as the ratio of the intensity of the transmitted light to the intensity of the incident light. The transmittance spectrum depends on the chemical and crystal structure, thickness and the surface morphology of the films, and depends on the important parameter effect on films' transmittance. Figure 2 shows the optical transmittance spectra as a function of wavelength of incident light for (PMMA–ZrO_2–Ag) nanocomposites. It is noticed from figure, the transmittance decreased with the increasing of the concentration for Ag nanoparticles. This is because of the agglomeration of nanoparticles with increasing concentration and increase of the number of charge carriers [82–86].

The size and shape distributions of the (PMMA–ZrO_2–Ag) nanocomposites were analysed using a scanning electron microscope (SEM). Figure 3 shows that the distribution of Ag nanoparticles in (PMMA–ZrO_2) nanocomposites at magnification power (×10). The optical microscope images expose that Ag nanoparticles are aggregated as a bunch at low ratios as shown in this figure, while, at high ratios, the presence of nanoparticles, which are uniformly distributed inside the (PMMA–ZrO_2) nanocomposites where charge carriers are allowed to pass through the paths [87–90].

Figure 4 shows the SEM images (PMMA–ZrO_2–Ag) nanocomposites. Scanning electron microscopy has been used to study the compatibility between various components of the polymers, Ag nanoparticles.

The films exhibit uniform density of grain distribution at surface morphology and surfaces morphology of the (PMMA–ZrO_2–Ag) nanocomposites show many aggregates or chunks randomly distributed of

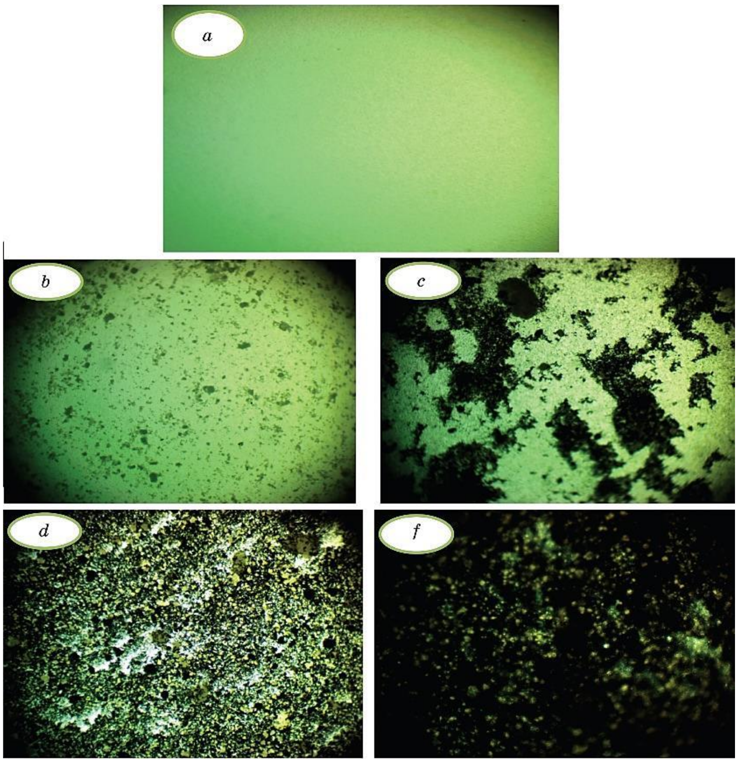

Fig. 3. Photo images (×10) for (PMMA–ZrO_2–Ag) nanocomposites: (*a*) for PMMA; (*b*) for (PMMA–ZrO_2); (*c*) for 2 wt.% Ag; (*d*) for 4 wt.% Ag; (*e*) for 6 wt.% Ag.

nanoparticles on the films' surface [91–94]. The results show an increase in the number of aggregations on the surface in accordance with increasing concentration of Ag nanoparticles [95].

From equation (3), it can be calculated the absorption coefficient α of nanocomposites. The variant of absorption coefficient for (PMMA–ZrO_2–Ag) as a function of photon energy of the incident light are presented in Fig. 5. It can be observe that absorption is comparatively small at low energy.

This means that the possibility of electron transition is low due to the energy of the incident photon not sufficient to move the electron from the valence band to the conduction band ($h\nu < E_g$) [96–100]. Absorption is high at high energies; this means that there is high possibility for electron transition, where the energy of incident photon is sufficient to transfer the electron from the valance band to the conduction band. This means that the energy of the incident photon is larger than the energy band gap. This shows that the absorption coefficient contribution is fig-

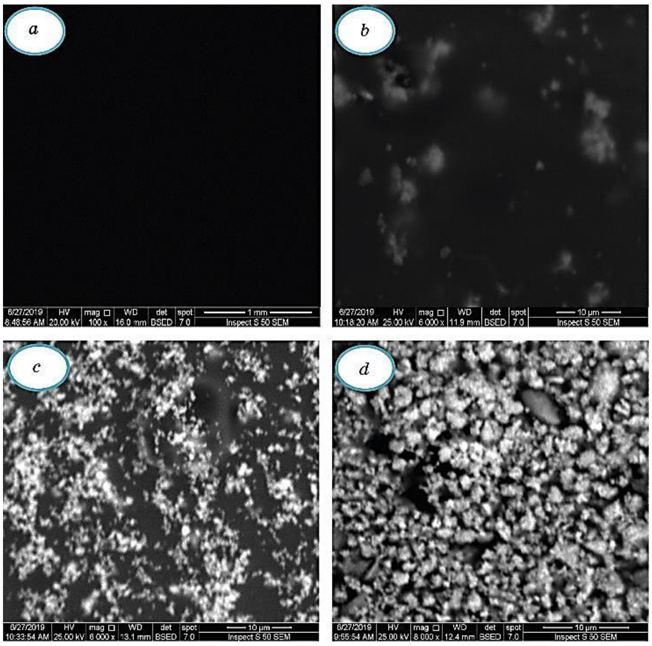

Fig. 4. SEM images (×10 µm) of (PMMA–ZrO$_2$–Ag) nanocomposites: (*a*) for PMMA; (*b*) for (PMMA–ZrO$_2$); (*c*) for 2 wt.% Ag nanoparticles, and (*d*) for 6 wt.% Ag nanoparticles.

uring out the nature of electron transition.

When the values in the absorption coefficient of material are high ($\alpha > 10^4$ cm^{-1}) at high energy, the electron transmission is possible to be direct transition of electron but the electron transmission will be possible to be indirect transition if the values of the absorption coefficient of material are typically low $\alpha < 10^4$ cm^{-1} at low energy.

The values of absorption coefficient of (PMMA–ZrO$_2$–Ag) nanocomposites are low $\alpha < 10^4$ cm^{-1}; the transition of electron is indirect. The absorption coefficient of nanocomposites increases with increasing of silver nanoparticles concentrations; this is because the increasing of number of charge carriers as shown in Fig. 5.

The absorption coefficient of (PMMA–ZrO$_2$–Ag) nanocomposites is less than 10^4 cm^{-1}; this clarifies that the electron transition is indirect [101].

Figures 6, 7 show the energies' gaps for allowed and forbidden indirect transitions of (PMMA–ZrO$_2$–Ag) nanocomposites. From these figures, we can observe that the energies gaps for allowed and forbidden indirect transitions of nanocomposites are decreased with the increasing of the Ag nanoparticles concentrations.

This behaviour is because of the creation of levels in the energy gap;

the transition of electron in this case is conducted in two stages that include the transition from the valence band to the local levels in energy gap and to the conduction band as a result of increasing the Ag nanoparticles concentrations; the electronic conduction depends on nanoparticles concentrations [102–104].

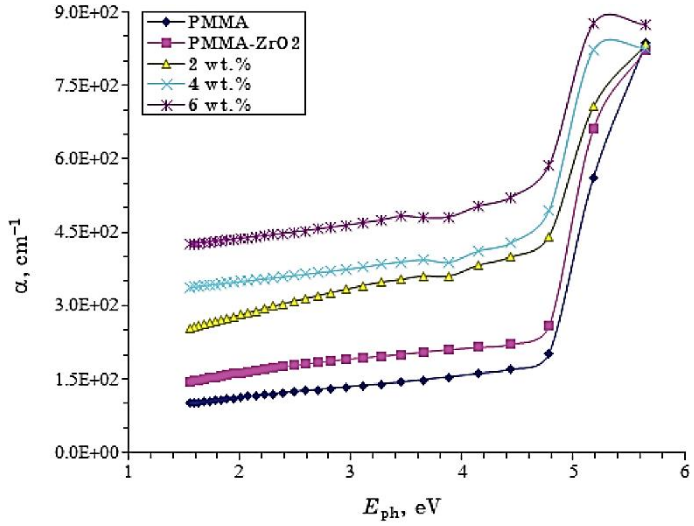

Fig. 5. Variation of absorption coefficient (α) for (PMMA–ZrO_2–Ag) nanocomposites with photon energy.

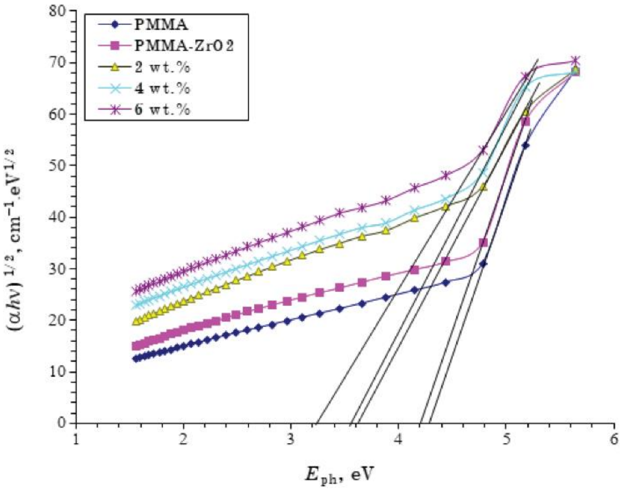

Fig. 6. Variation of $(\alpha h\nu)^{1/2}$ for (PMMA–ZrO_2–Ag) nanocomposites with photon energy.

Figure 8 shows the extinction coefficient variant as a function of wavelength for the (PMMA–ZrO_2–Ag) nanocomposites. The figure shows that the extinction coefficient k of (PMMA–ZrO_2–Ag) nanocomposites increase with increasing of the silver nanoparticles concentration; this is due to the increasing in optical absorption and photons dispersion in the (PMMA–ZrO_2–Ag) nanocomposites. The extinction coefficient of nanocomposites has high values in UV region; this behaviour attributed to high absorbance of all samples of nanocomposite.

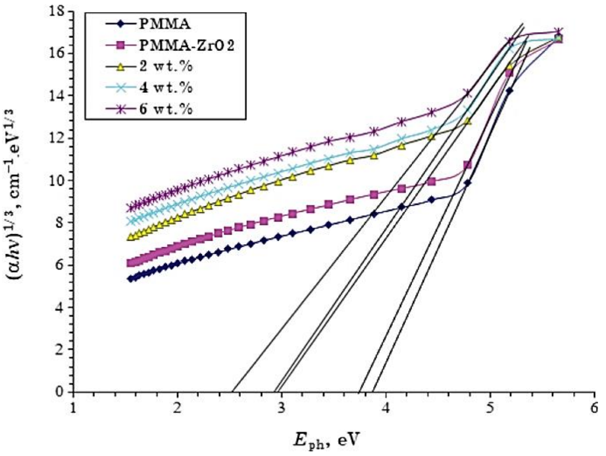

Fig. 7. Variation of $(\alpha h\nu)^{1/3}$ for (PMMA–ZrO_2–Ag) nanocomposites with photon energy.

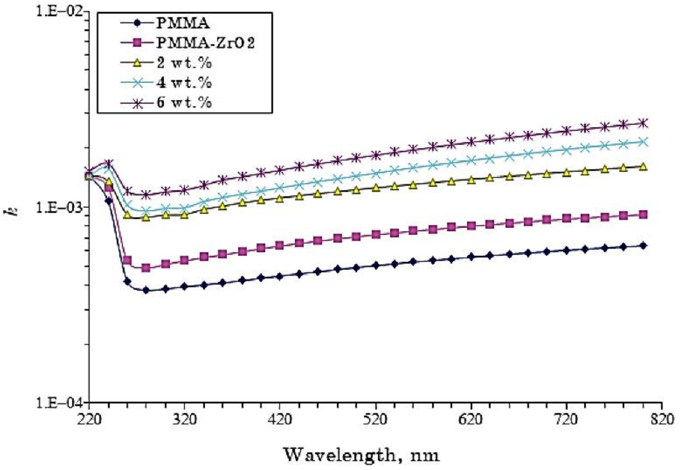

Fig. 8. Variation of extinction coefficient for (PMMA–ZrO_2–Ag) nanocomposites with wavelength.

In addition, extinction coefficient of nanocomposites increases with the increasing of the wavelength at visible and near infrared regions, which attributed to the absorption coefficient of (PMMA–ZrO_2–Ag) nanocomposites is approximately constant at visible and near-infrared regions; hence, the extinction coefficient increases with the increasing of the wavelength according to Eq. (8) [105].

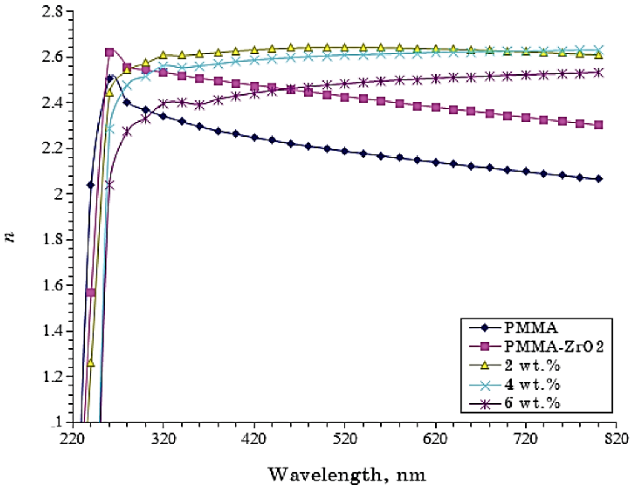

Fig. 9. Variation of refractive index for (PMMA–ZrO_2–Ag) nanocomposites with wavelength.

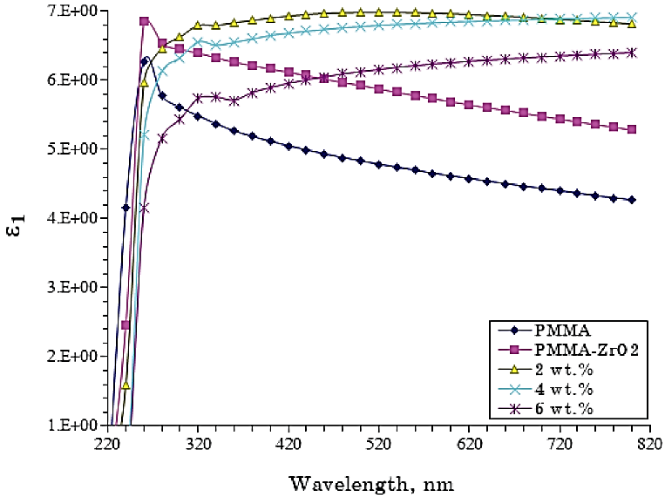

Fig. 10. Real dielectric constant as a function of wavelength for (PMMA–ZrO_2–Ag) nanocomposites.

The refractive index can be calculated by using Eq. (5). Figure 9 shows the refractive index n as a function of wavelength; it is clear from figure, the refractive index of nanocomposites increases with the increasing of the silver nanoparticles concentrations, such as refractive index is decreased with the increase of the wavelength. This recital attributed to the density of nanocomposites. When the incident light interacts with a sample, it has high refractivity at UV region; hence, the values of refractive index will be increased [106–108].

The real dielectric constant (ε_1) and imaginary (ε_2) dielectric constant connected to the refractive index (n) and extinction coefficient (k) values. From equations (9) and (10), it can be measured the values of ε_1 and ε_2 dielectric constant respectively. The real (ε_1) and imaginary (ε_2) parts of dielectric constant as functions of wavelength for (PMMA–ZrO_2–Ag) nanocomposites are shown in Figs. 10 and 11, correspondingly. The ε_1 dielectric constant depends on n^2 and k^2, but ε_2 dielectric constant depends on n and k [109]. The figures show that the real and imaginary parts of dielectric constant are increased with the increase of Ag nanoparticles' concentration. The increase of real and imaginary parts of dielectric constant with Ag nanoparticles concentration is because of the increase of refractive index and extinction coefficient. As shown in these figures, the real and imaginary parts of dielectric constant of (PMMA–ZrO_2–Ag) nanocomposites are changed with the wavelength; this is due to the real part of dielectric constant depending on refractive index. Due to this fact, effect of extinction coefficient is very small, and the imaginary part of dielectric constant depends on extinction coefficient especially in the visible and near-infrared regions of wavelength where the refractive index is approximately constant while extinction coefficient increases with the increase of the wavelength [110].

Figure 12 shows the variation of optical conductivity with the wavelength of nanocomposites. The figure shows that the optical conductivity of all samples of nanocomposites are decreased with the increasing of the wavelength; this behaviour is attributed to the optical conductivity depends strongly on the wavelength of the radiation incident on the samples of (PMMA–ZrO_2–Ag) nanocomposites. The increasing of optical conductivity at low wavelength of photon is because of high absorbance of all samples of nanocomposites in that region and, therefore, increasing of the charge transfer excitations. The optical conductivity spectra indicated that the samples are transmittance within the visible and near infrared regions. Too, the optical conductivity of nanocomposites is increased with the increase of Ag nanoparticles' concentration; this behaviour is related to the creation of localized levels in the energy gap; the increase of Ag nanoparticles' concentration increases the density of localized stages in the band structure, hence, increase of the absorption coefficient consequently increasing the op-

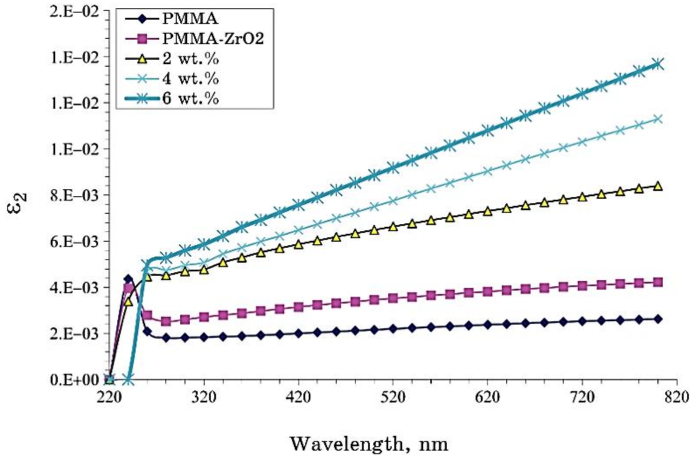

Fig. 11. Imaginary dielectric constant as a function of wavelength for (PMMA–ZrO_2–Ag) nanocomposites.

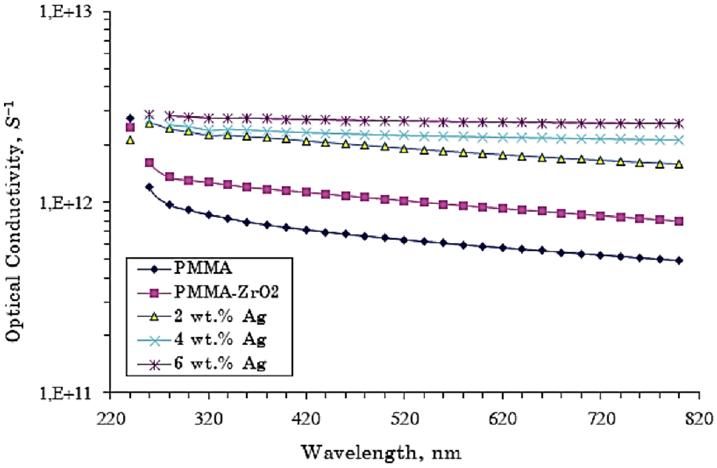

Fig. 12. Variation of optical conductivity for (PMMA–ZrO_2–Ag) nanocomposites with wavelength.

tical conductivity of (PMMA–ZrO_2–Ag) nanocomposites [111, 112].

4. CONCLUSION

The optical properties, which include absorbance, absorption coefficient, extinction coefficient, refraction index, optical conductivity, real and imaginary part of the (PMMA–ZrO_2) nanocomposites, are increased with increase in sliver nanoparticles' concentration.

The optical transmittance and energy gap for indirect transition (allowed, forbidden) are decreased with increasing the concentration of the silver nanoparticles.

The obtained results show that the (PMMA/$ZrO_{2/}$Ag) nanocomposites may be used for different medical and industrial applications.

REFERENCES

1. N. L. Singh, A. Qureshi, F. Singh, and D. K. Avasthi, *Mater. Sci. Eng.*, **137**: 85 (2007).
2. R. K. Y. Fu, I. T. L. Cheung, Y. F. Mei, C. H. Shek, G. G. Siu, P. K. Chu, W. M. Yang, Y. X. Leng, Y. X. Huang, X. B. Tian, and S. Q. Yang, *Nucl. Instrum. Methods Phys. Res., Sect. B*, **237**: 417 (2005).
3. H. Kaczmarek and H. Chaberska, *Appl. Surf. Sci.*, **252**: 8185 (2006).
4. F. Yakuphanoglu, G. Barim, and I. Erol, *Physica*, 391: 136 (2007).
5. B. M. Novak, *Advanced Materials*, **5**, No. 6: 422 (1993).
6. U. Schubert, N. Husing, and A. Lorenz, *Chem. Mater.*, **7**: 1995 (2010).
7. J. Wen and G. L. Wilkes, *Chem. Mater.*, **8**: 1667 (1996).
8. Z. H. Huang and K. Y. Oiu, *Polym. Bull.*, **35**: 607 (1995).
9. H. T. Wang, P. Xu, W. Zhong, L. Shen, and Q. Du, *Polym. Degrad. Stabil.*, **87**: 319 (2005).
10. T. Otsuka and Y. Chujo, *Polym. Journal*, **42**: 58 (2010).
11. V. G. Konakove et al., *Rev. Adv. Mater. Sci.*, **13**: 71 (2016).
12. R. C. Garvie, R. H. Hannink, and R. T. Pascoe, *Nature*, **258**: 703 (1975).
13. R. H. Hannink, P. M. Kelly, and B. C. Muddle, *J. Am. Ceram. Soc.*, **83**: 461 (2000).
14. S. Tekeli, M. Erdogan, and B. Aktas, *Ceram. Int.*, **30**: 2203 (2004).
15. D. Ai and S. Kang, *Ceram. Int.*, **30**: 619 (2004).
16. S. R. Choi and N. P. Bansal, *Ceram. Int.*, **31**: 39 (2005).
17. Y. Zhang, J. Chen, L. Hu, and W. Liu, *Mater. Lett.*, **60**: 2302 (2006).
18. B. Istrate, C. Munteanu, M. N. Matei, B. Oprisan, D. Chicet, and K. Earar, *International Conference on Innovative Research 2016—ICIR Euroinvent 2016. IOP Conf. Series: Materials Science and Engineering* (IOP Publishing: 2016), p. 133.
19. M. T. Byrene, W. P. McNamee, and Y. K. Gun'ko, *Nanotechnology*, **19**: 415707 (2008).
20. D. R. Askeland and P. P. Fulay, *Essential of Materials Science and Engineering* (New York: 2010).
21. R. A. Pearson and A. F. Yee, *Polymer*, **34**: No. 17: 3858 (1993).
22. M. Nanda and D. K. Tripathy, *Express Polymer Letters*, **2**: 855 (2008).
23. A. B. Panda, A. Pathak, and P. Pramanik, *Material Letters*, **52**: 180 (2002).
24. Y. G. Suu, *Studies on Mechanical Properties of Poly (Methayl Methacrylate) — Modified Natural Rubber Blend (September, 2008).*
25. R. A. Pearson and A. F. Yee, *Polymer*, **34**, No. 17: 3858 (1993).
26. N. Hameed, S. P. Thomas, R. Abraham, and S. Thomas, *Express Polymer Letters*, **1**: 345 (2007).
27. J. F. Rebek, *Experimental Methods in Polymer Chemistry* (New York: John Wiley and Sons: 1980).

28. A. Hashim and A. Hadi, *Sensor Letters*, **15**: (2017); doi:10.1166/sl.2017.3900
29. A. Hashim and Q. Hadi, *Journal of Inorganic and Organometallic Polymers and Materials*, **28**, Iss. 4: 1394 (2018); https://doi.org/10.1007/s10904-018-0837-4
30. A. Hashim, Y. Al-Khafaji, and A. Hadi, *Transactions on Electrical and Electronic Materials*, (2019); https://doi.org/10.1007/s42341-019-00145-3
31. A. Hadi and A. Hashim, *Ukrainian Journal of Physics*, **62**, No. 12 (2017); doi: 10.15407/ujpe62.12.1044
32. I. R. Agool, K. J. Kadhim, and A. Hashim, *International Journal of Plastics Technology*, **21**, Iss. 2 (2017); https://doi.org/10.1007/s12588-017-9192-5
33. A. Hashim and N. Hamid, *Journal of Bionanoscience*, **12**, No. 6 (2018); doi:10.1166/jbns.2018.1591
34. A. Hashim and Z. S. Hamad, *Journal of Bionanoscience*, **12**, No. 4 (2018); doi:10.1166/jbns.2018.1551
35. D. Hassan and A. Hashim, *Journal of Bionanoscience*, **12**, Iss. 3 (2018); doi:10.1166/jbns.2018.1537
36. A. Hashim and Z. S. Hamad, *Journal of Bionanoscience*, **12**, No. 4 (2018); doi:10.1166/jbns.2018.1561
37. B. Abbas and A. Hashim, *International Journal of Emerging Trends in Engineering Research*, **7**, No. 8 (2019); https://doi.org/10.30534/ijeter/2019/06782019
38. K. H. H. Al-Attiyah, A. Hashim, and S. F. Obaid, *Journal of Bionanoscience*, **12** (2018); doi:10.1166/jbns.2018.1526
39. K. J. Kadhim, I. R. Agool, and A. Hashim, *Materials Focus*, **5**, No. 5 (2016); https://doi.org/10.1166/mat.2016.1371
40. K. J. Kadhim, I. R. Agool, and A. Hashim, *Journal of Advanced Physics*, **6**, No. 2 (2017); https://doi.org/10.1166/jap.2017.1313
41. A. Hashim, I. R. Agool, and K. J. Kadhim, *Journal of Bionanoscience*, **12**, No. 5 (2018); doi:10.1166/jbns.2018.1580
42. F. L. Rashid, S. M. Talib, A. Hadi, and A. Hashim, *IOP Conf. Series: Materials Science and Engineering*, **454**: 012113 (2018); doi:10.1088/1757-899X/454/1/012113
43. A. Hadi, F. L. Rashid, H. Q. Hussein, and A. Hashim, *IOP Conference Series: Materials Science and Engineering*, **518**, Iss. 3: 5 (2019); doi:10.1088/1757-899X/518/3/032059
44. I. R. Agool, K. J. Kadhim, and A. Hashim, *International Journal of Plastics Technology*, **21**, Iss. 2 (2017); https://doi.org/10.1007/s12588-017-9196-1
45. A. Hadi, A. Hashim, and D. Hassan, *Bulletin of Electrical Engineering and Informatics*, **9**, No. 1 (2020); doi:10.11591/eei.v9i1.1323
46. A. S. Shareef, F. L. Rashid, A. Hadi, and A. Hashim, *International Journal of Scientific & Technology Research*, **8**, Iss. 11 (2019).
47. F. Ali Jasim, A. Hashim, A. G. Hadi, F. Lafta, S. R. Salman, and H. Ahmed, *Research Journal of Applied Sciences*, **8**, Iss. 9: 439 (2013).
48. F. Ali Jasim, F. Lafta, A. Hashim, M. Ali, and A. G. Hadi, *Journal of Engineering and Applied Sciences*, **8**, No. 5: 140 (2013).
49. I. R. Agool, F. S. Mohammed, and A. Hashim, *Advances in Environmental Biology*, **9**, No. 11 (2015).
50. F. L. Rashid, A. Hashim, M. Ali Habeeb, S. R. Salman, and H. Ahmed,

Journal of Engineering and Applied Sciences, **8**, No. 5: 137 (2013).
51. A. Hashim, H. Abduljalil, and H. Ahmed, *Egypt. J. Chem.* (2019); doi:10.21608/EJCHEM.2019.7154.1590
52. A. Hashim, M. A. Habeeb, A. Khalaf, and A. Hadi, *Sensor Letters*, **15**: 589 (2017); doi:10.1166/sl.2017.3856
53. S. Hadi, A. Hashim, and A. Jewad, *Australian Journal of Basic and Applied Sciences*, **5**, No. 9: 2192 (2011).
54. Q. M. Jebur, A. Hashim, M. A. Habeeb, *Transactions on Electrical and Electronic Materials* (2019); https://doi.org/10.1007/s42341-019-00121-x
55. H. Abduljalil, A. Hashim, and A. Jewad, *Journal of Scientific Research*, **63**, No. 2: 231 (2011).
56. A. Hashim and A. Hadi, *Ukrainian Journal of Physics*, 62, No. 12 (2017); doi:10.15407/ujpe62.12.1050
57. A. Hashim and A. Hadi, *Ukrainian Journal of Physics*, **63**, No. 8 (2018); https://doi.org/10.15407/ujpe63.8.754
58. A. Hashim and Q. Hadi, *Sensor Letters*, **15**: (2017); doi:10.1166/sl.2017.3892
59. A. Hashim, M. Ali Habeeb, A. Hadi, Q. M. Jebur, and W. Hadi, *Sensor Letters*, **15** (2017); doi:10.1166/sl.2018.3935
60. A. Hashim and Z. S. Hamad, *J. Nanostruct.*, **9**, No. 2: 340 (2019); doi:10.22052/JNS.2019.02.016
61. D. Hassan, A. H. Ah-Yasari, *Bulletin of Electrical Engineering and Informatics*, **8**, Iss. 1 (2019); doi:10.11591/eei.v8i1.1019
62. M. Ali Habbeb, A. Hashim, and A.-R. K. AbidAli, *European Journal of Scientific Research*, **61**, No. 3: 367 (2011).
63. D. Greenaway and G. Harbeke, *Optical Properties and Band Structure of Semiconductors* (New York: Pergamon Press: 1966).
64. B. H. Rabee and A. Hashim, *European Journal of Scientific Research*, **60**: No. 2: 247 (2011).
65. A. Hazim, H. M. Abduljalil, and A. Hashim, *International Journal of Emerging Trends in Engineering Research*, **7**, No. 8 (2019); https://doi.org/10.30534/ijeter/2019/04782019
66. W. Klopffer, *Introduction to Polymer Spectroscopy* (Springer: 1984).
67. H. A. Macleod, *Thin Film Optical Filter* (New York: McGraw Hill: 2001).
68. A. Ahmed, A. Awatif, and A. Zeid, *J. Eng. and Technology*, **25**: No. 4: 137 (2007).
69. A. J. Kareem, M. H. Aliand, and K. A. Ali, *RRPL*, **6**, No. 2: 071-082 (2015).
70. P. Samarasekara and U. Wijesinghe, *GESJ: Phys.*, **2**: 14 (2015).
71. J. H. Nahida and R. E. Marwa, *Eng. & Tech. J.*, **29**: 4 (2011).
72. S. D. Hutagalwng and B. Y. Lee, *Proceeding of the 2nd International Conference 'Nano/Micro Engineered and Molecular Systems' (January, 2007)* (Bangkok, Thailand: 2007).
73. E. Tang, G. Cheng, and X. Ma, *Powder Technology*, **161**: 209 (2006).
74. S. Hussein, *Study the Optical and Mechanical Properties of (PMMA–TiO$_2$) Nanocomposite* (M.Sc. Thesis) (Babylon: Collage of Science, Babylon University: 2014).
75. P. Phukan and D. Saikia, *Int. J. Photoenergy*, **2013**: 728280 (2013).
76. A. Hashim and Q. Hadi, *Journal of Materials Science: Materials in Electronics*,

29: 11598 (2018); https://doi.org/10.1007/s10854-018-9257-z
77. A. H. O. Alkhayatt, A. H. Al-Azzawi, and Z. Alakayashi, *IOSR Journal of Applied Physics*, **8**, No. 1: 11 (2016).
78. A. Hazim, H. M. Abduljalil, and A. Hashim, *Transactions on Electrical and Electronic Materials* (2019); https://doi.org/10.1007/s42341-019-00148-0
79. K. Al-Ammar, A. Hashim, and M. Husaien, *Chemical and Materials Engineering*, **1**, No. 3 (2013); doi:10.13189/cme.2013.010304
80. A. H. Ahmad, A. M. Awatif, and N. Z. Abdul-Majied, *J. of Eng. & Technology*, **25**: No. 4: 558 (2007).
81. K. Rtintu, K. Saurav, K. Sulakshnab, and V. Nampoori, *J. Non-Oxide Glasses*, **2**, No. 4: 167 (2010).
82. A. Hazim, A. Hashim, H. M. Abduljalil, *International Journal of Emerging Trends in Engineering Research*, **7**, No. 8 (2019); https://doi.org/10.30534/ijeter/2019/01782019
83. J. Ramesh Babu and K. Vijaya Kumar, *International Journal of Chemistry Technology Research*, **7**, No. 1: 171 (2014).
84. Z. H. E. M. Ghanipour and D. Dorranian, *Journal of Theoretical Applied Physics*, **8**, No. 139: 117 (2014).
85. A. Hashim and A. Jassim, *Journal of Bionanoscience*, **12**: (2018); doi:10.1166/jbns.2018.1518
86. A. Hashim and A. Jassim, *Sensor Letters*, **15**, No. 12 (2017); doi:10.1166/sl.2018.3915
87. H. Ahmed, H. M. Abduljalil, and A. Hashim, *Transactions on Electrical and Electronic Materials* (2019); https://doi.org/10.1007/s42341-019-00100-2
88. E. Yousif, M. Abdallh, H. Hashim, N. Salih, J. Salimon, and B. M. Abdullah, *International Journal of Industrial Chemistry*, **4**, No. 4: 1 (2013).
89. A. Hashim and A. Hadi, *Sensor Letters*, **15**: (2017); doi:10.1166/sl.2017.3910
90. Z. Al-Ramadhan, A. Hashim, and A. J. Kadham Algidsawi, *AIP Conference Proceedings*, **1400**, No. 1 (2011); https://doi.org/10.1063/1.3663109
91. A. Hashim, M. Ali Habeeb, and A. Hadi, *Sensor Letters*, **15**, No. 9: 758 (2017); doi:10.1166/sl.2017.3876
92. A. Hashim and M. Ali Habeeb, *Transactions on Electrical and Electronic Materials* (2019); doi:10.1007/s42341-018-0081-1
93. A. Hashim and A. Hadi, *Ukrainian Journal of Physics*, **62**, No. 11 (2017); doi:10.15407/ujpe62.11.0978
94. N. H. Al-Garah, F. L. Rashid, A. Hadi, and A. Hashim, *Journal of Bionanoscience*, **12** (2018); doi:10.1166/jbns.2018.1538
95. W. A. Al-Dulaimi, *International Journal of Physics and Applications*, **8**, No. 1: 25 (2016).
96. D. Hassan and A. Hashim, *Journal of Bionanoscience*, **12**, Iss. 3 (2018); doi:10.1166/jbns.2018.1537
97. O. G. Abdullah, *European Scientific Journal*, **10**, No. 33 (2014).
98. D. Hassan and A. Hashim, *Journal of Bionanoscience*, **12**, Iss. 3 (2018); doi:10.1166/jbns.2018.1533
99. A. Hashim, K. H. H. Al-Attiyah, and S. F. Obaid, *Ukrainian Journal of Physics*, **64**, No. 2 (2019); https://doi.org/10.15407/ujpe64.2.157
100. K. H. H. Al-Attiyah, and A. Hashim, *International Journal of Plastics Technology*, **23**, No. 1 (2019); https://doi.org/10.1007/s12588-019-09228-5

101. T. Hamad, R. Yusop, W. Al-Taa'y, B. Abdullah, and E. Yousif, *International Journal of Polymer Science*, **8** (2014).
102. V. Sangawar and M. Golchha, *International Journal of Scientific & Engineering Research*, **4**: 6 (2013).
103. O. Abdullah, D. A. Tahir, S. S. Ahmad, and H. T. Ahmad, *Journal of Applied Physics*, **4**: 52 (2013).
104. E. A. Davis and N. F. Mott, *Philos. Mag.*, **22**: 903 (1970).
105. J. Tauc, A. Menth, and D. Wood, *Phys. Rev. Lett.*, **25**: 749 (1970).
106. R. Tintu, K. Saurav, K. Sulakshn, V. Nampoori, Radhakrishnan, and S. Thomas, *Journal of Non-Oxide Glasses*, **2**, No. 4: 167 (2010).
107. O. Gh. Abdullah, B. K. Aziz, and D. M. Salh, *Indian Journal of Applied Research*, **3**, No. 11: 477 (2013).
108. M. Venkatarayappa, S. Kilarkaje, A. Prasad, and D. Hundekal, *Journal of Materials Science and Engineering*, **1**: 964 (2011).
109. H. Ahmed, A. Hashim and H. M. Abduljalil, *Egypt. J. Chem.*, **62**, No. 4: 1167 (2019); doi:10.21608/EJCHEM.2019.6241.1522
110. A. Hashim, I. R. Agool, and K. J. Kadhim, *Journal of Materials Science: Materials in Electronics*, **29**, Iss. 12: 10369 (2018); https://doi.org/10.1007/s10854-018-9095-z
111. H. Ahmed, H. M. Abduljalil, and A. Hashim, *Transactions on Electrical and Electronic Materials* (2019); https://doi.org/10.1007/s42341-019-00111-z
112. O. Abdullah, D. R. Saber, and L. O. Hamasalih, *Universal Journal of Materials Science*, **3**, No. 1: 1 (2015).